Photoelectron emission microscopy observation of inversion domain boundaries of GaN-based lateral polarity heterostructures

Cite as: Journal of Applied Physics **94**, 5720 (2003); https://doi.org/10.1063/1.1618355
Submitted: 01 May 2003 • Accepted: 19 August 2003 • Published Online: 23 October 2003

W.-C. Yang, B. J. Rodriguez, M. Park, et al.

Photoelectron emission microscopy observation of inversion domain boundaries of GaN-based lateral polarity heterostructures

W.-C. Yang, B. J. Rodriguez, M. Park, and R. J. Nemanich[a)]
Department of Physics, and Materials Science and Engineering, North Carolina State University, Raleigh, North Carolina 27695

O. Ambacher and V. Cimalla
Center for Micro- and Nanotechnologies, Technical University Ilmenau, Ilmenau, Germany

(Received 1 May 2003; accepted 19 August 2003)

An intentionally grown GaN film with laterally patterned Ga- and N-face polarities is studied using *in situ* UV-photoelectron emission microscopy (PEEM). Before chemical vapor cleaning of the surface, the emission contrast between the Ga- and N-face polarities regions was not significant. However, after cleaning the emission contrast between the different polarity regions was enhanced such that the N-face regions exhibited increased emission over the Ga-face regions. The results indicate that the emission threshold of the N-face region is lower than that of the Ga face. Moreover, bright emission was detected from regions around the inversion domain boundaries of the lateral polarity heterostructure. The PEEM polarity contrast and intense emission from the inversion domain boundary regions are discussed in terms of the built-in lateral field and the surface band bending induced by the polarization bound surface charges. © *2003 American Institute of Physics.* [DOI: 10.1063/1.1618355]

I. INTRODUCTION

An important property of wurtzite GaN is its large spontaneous and piezoelectric polarization, which strongly affects the electrical and optical properties of GaN-based heterostructure devices.[1,2] A gradient in the polarization induces bound surface charges and creates strong internal electric fields in the film. The sign of the bound charges at the surface and the direction of the field depend on the orientation of the polarization, which is determined by film polarity; Ga or N face. A GaN film with Ga-face polarity is designated [0001] orientation while N-face polarity is designated [000-1] orientation.[3] The built-in field induced by the polarization can modify the energy bands at the surface, leading to surface band bending.[4]

Recently, intentionally grown GaN-based lateral polarity heterostructures (LPHs), in which Ga- and N-face regions were grown laterally on the same surface and separated by inversion domain boundaries (IDBs), have become of interest for potential application in optoelectric devices.[1,2] In particular, it has been proposed that an IDB can be employed as a tunnel junction barrier between regions with two-dimensional electron gases (2DEGs) in a lateral GaN/AlGaN/GaN heterostructure.[2]

The spontaneous and piezoelectric polarization of the GaN leads to a polarization bound charge at the surface and interface. The Ga-face surface exhibits a negative bound charge, and the N-face surface exhibits a positive bound charge. These charges are screened by free carriers and ionized donors in the bulk of the *n*-type GaN, and by charges in the surface and interface states. The band bending at the GaN surfaces is expected to be upward for the Ga-face regions and downward for the N-face regions, which will lead to a built-in field along the surface in the region of the IDB.[5]

Although the IDB has been studied theoretically,[6] the structural and electrical properties have not been studied in detail. While the IDB is expected to exhibit atomic scale dimensions, the built-in lateral field is expected to vary over a larger range of up to μm from the IDB. In addition, during film growth a morphological and structural transition region will also be created near the IDB.[7] We will term this larger region, which includes all of these effects, as the inversion domain boundary region (IDBR). The optical properties of the inversion domain boundary region were investigated by photoluminescence measurements.[8] Bright emission was observed in the IDBR, and it was suggested that it originated from shallow, optically active traps.[5,8] Previously, we also examined the surfaces of a LPH using piezoresponse force microscopy (PFM) and Raman scattering.[9,10] A slightly higher piezoresponse observed for the N-face regions was associated with a larger total polarization and the correspondingly larger bound surface charge.[9] This was consistent with Raman measurements of the relative peak shifts across the IDBR.[10] The measurements indicated that the N-face region is under less compressive stress, which implies a smaller piezoelectric polarization and a larger total polarization for the N face.

In this study, the IDBR of a GaN-based LPH is explored using UV photoelectron emission microscopy (UV-PEEM). PEEM is an emission microscopy technique in which images of a material surface are formed by photoexcited electrons.[11] In this technique the surface is uniformly illuminated with UV light, and the photoemitted electrons are imaged with electron optics. In our experiments, the UV light is near the threshold for photoelectric emission. In UV-PEEM the image

a)Electronic mail: robert_nemanich@ncsu.edu

contrast originates from variation in the photoelectric yield, where the density of states and the photoelectric threshold both affect the PEEM image contrast. In metals, the photoelectric threshold is the work function while for semiconductors the photoelectric threshold is dependent on the electron affinity, the band gap, and the doping. The band bending can also contribute to the photoelectric yield with enhanced emission for downward band bending.[11,12]

For the different polarity surfaces we expect to find significant differences in band bending. This will lead to differences in the free carrier density in the near-surface region with electrons accumulated in the conduction band of the N-face regions. Moreover, recent studies of metal contacts on Ga- and N-polarity surfaces indicate substantially different Schottky barrier heights. These results suggest that the electron affinity of the different surfaces can be different. The electron affinity of a semiconductor is a function of the surface dipole, and the different bonding of the Ga- and N-polarity surfaces could result in different surface dipole terms and consequently different electron affinities.[13]

This study will establish how these effects are manifested in PEEM images of GaN films with different local polarities. The experiments will explore how image contrast can reflect the electronic structure of the different polar surfaces. With tunable UV FEL we can obtain images with controlled photoexcitation to maximize the PEEM image contrast and to determine the photothresholds of local regions of the GaN film surface.

Here, we report PEEM observations of polarity contrast and local intensity enhancement in GaN films. We find a higher photoyield from the N-face regions compared with the Ga-face regions. In particular, a strongly enhanced emission intensity and a photothreshold reduction is observed in the region of the IDB. We propose an energy band variation in the IDBR and suggest that the significantly higher photoyield is attributed to charge accumulation at the IDB.

II. EXPERIMENT

The experiments were performed in an UV-PEEM system that is connected via a UHV sample transfer system to a custom gas source molecular beam epitaxy (GSMBE) system. The photoelectrons were excited with UV-light from the tunable UV free electron laser (FEL) at Duke University. The base pressure of the PEEM system was below 5×10^{-10} Torr.

The GaN film with laterally patterned Ga- and N-face polarities was fabricated using plasma induced molecular beam epitaxy (PIMBE). The Ga-face GaN (1 μm thick) was grown on an AlN nucleation layer (10 nm thick), while the N-face GaN (1 μm thick) was grown directly on the sapphire substrate. The IDBs are created at the boundaries between the Ga- and N-face GaN. The details of the growth processing can be found elsewhere.[7,14] The free electron concentration was determined to be $N_d=4.1\times10^{17}$ cm^{-3} for the N-face region and 2.5×10^{17} cm^{-3} for the Ga-face region by Raman scattering measurements.[10]

Prior to loading, the film was degreased sequentially in trichloroethylene, acetone, and methanol baths for 10 min each. After *ex situ* cleaning, the film was loaded into the UHV-GSMBE chamber (base pressure of 3×10^{-10} Torr) for an ammonia-based high-temperature chemical vapor clean (CVC) to remove oxygen and carbon contaminants on the film.[15,16] Oxygen contamination is removed by thermal desorption, and carbon contamination removed by reaction with NH_3. The sample was initially heated to 600 ± 20 °C, and the ammonia vapor was initiated. The sample was then heated to 800 ± 20 °C and held for 15 min at a pressure of 1×10^{-5} Torr. Upon completion of the CVC process, the sample was cooled under the flow of ammonia. The ammonia flow was terminated below 600 °C. When the temperature reached ~150 °C, the sample was transferred in UHV to the PEEM chamber.

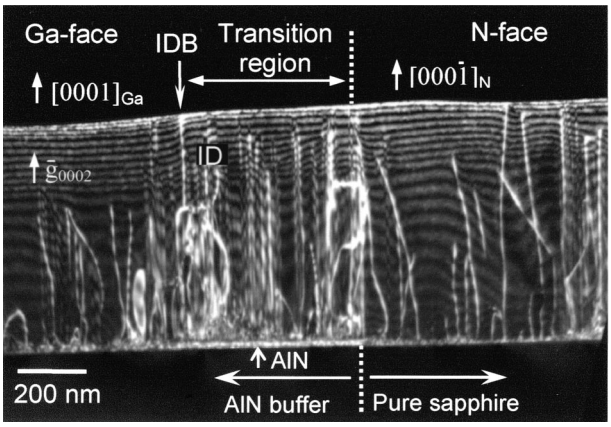

FIG. 1. Cross section TEM micrograph of a GaN film with laterally patterned Ga- and N-face polarities fabricated using PIMBE. The N-face region extends over the AlN buffer layer to the IDB.

The film surface was explored before and after *in situ* cleaning, and PEEM images were obtained with photon energies from 4.5 to 6.3 eV. The spontaneous radiation of the FEL is pulsed with a repetition rate of 15 MHz and a pulse duration of ~300 ps. The average FEL power was ~2 mW which was focused to approximately 20 W/cm^2. The typical output spectrum of the FEL is nearly Gaussian with a full width at half maximum of ~0.1 eV. The capabilities of the PEEM-FEL are described in more detail elsewhere.[11]

The lateral resolution in the PEEM is limited by aberrations associated with the necessary accelerating field and the average emission energy and energy spread of the emitted electrons.[17] In the UV-FEL PEEM, the electric potential used for accelerating the electrons is ~20 kV across a gap of 2 mm, and the tunable UV-FEL light minimizes the energy spread of the emitted electrons, which system allows ~10 nm imaging.[11] PEEM images are enhanced with a microchannel plate and displayed on a phosphor screen. The images were observed with a CCD camera, and stored digitally with an image processor. For the data presented here, 16 successive frames were integrated to form an image.

III. RESULTS

Figure 1 presents a cross section TEM image of a region of the inversion domain boundary of a GaN LPH.[7] The left side of the IDB was identified as the Ga-face region while

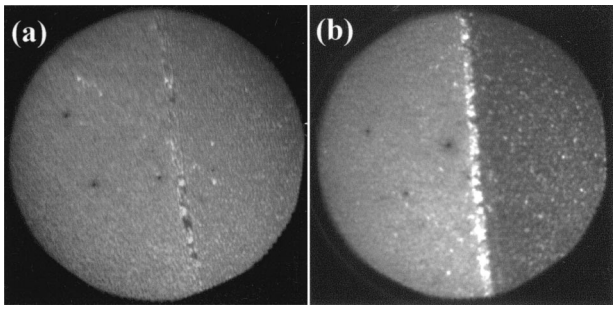

FIG. 2. PEEM images of a GaN-based lateral polarity heterostructure (a) before the CVC process and (b) after the CVC process. The field of view is 50 μm, and the FEL photon energy is 5.4 eV.

the right side as the N-face region. The IDB was expected to be located at the edge of the patterned AlN buffer layer. However, it is apparent that the IDB is shifted by several 100 nm towards the Ga-face region. The structural transition region is evident as the N-face layer that has formed over the patterned AlN buffer layer. This structural transition region exhibits a slightly higher density of threading dislocations than in the nearby Ga- and N-face regions.

Figure 2 displays PEEM images of the GaN film with laterally different polarities before and after *in situ* cleaning. For the as-loaded GaN surface, the brightness contrast between the Ga- and N-face regions is not apparent, and the emission from the boundary regions is only slightly more intense than the other regions [Fig. 2(a)]. For photon energies from 5.0 to 6.3 eV, the contrast did not change, but the whole surface became slightly brighter at higher photon energies. This indicates that the photoelectron yield of the as-loaded GaN surface is independent of the surface polarity.

However, after the cleaning process, the contrast between the different polarity regions was significantly enhanced [Fig. 2(b)]. Through comparison of high magnification PEEM and AFM topography images shown in Fig. 3, we could identify the polarity of the specific surface regions. The darker region in the PEEM is recognized as a Ga-face surface while the brighter region is a N-face surface. In addition, as displayed in Figs. 2 and 3, relatively stronger emission intensity was detected from the inversion domain boundary regions.

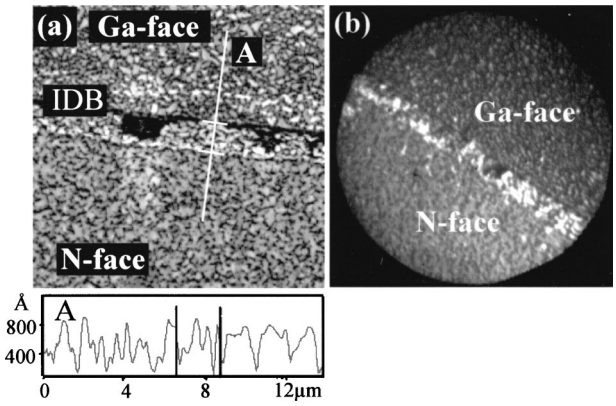

FIG. 3. (a) AFM image (scan size of $20\times20\ \mu m^2$) of the GaN lateral polarity heterostructure and a cross-section profile along the indicated line; (b) PEEM image (20 μm field of view) obtained with a photon energy of 5.6 eV.

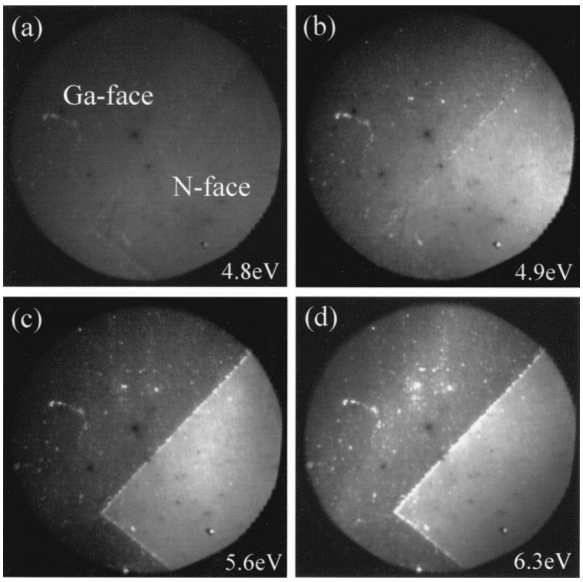

FIG. 4. PEEM images of the CVC-cleaned GaN film showing the lateral polarity heterostructure. The images were obtained with photon energies of (a) 4.8 eV, (b) 4.9 eV, (c) 5.6 eV, and (d) 6.3 eV, respectively. The field of view is 150 μm.

The AFM topography image displays the apparent region extended from the IDB to the N-face side with a width of $\sim$2 μm [Fig. 3(a)]. The solid line that crosses the IDBR has hatchmarks that indicate the IDB location and the suggested extent of the IDBR. The origin of this topography that distinguishes the IDBR is still uncertain. In consideration of the surface electrical structure near the IDB, we expect that the IDBR is extended beyond the IDB to each face side. As indicated from the cross section TEM (Fig. 1) and XRD studies[7] of similar films, a structural transition region is present which extends from the IDB towards the N-face side. The AFM measurements confirm that the morphology associated with the N-face region extends to the IDB. It is interesting to note that the intense emission in the PEEM was only observed from the N-face side of the IDBR [Fig. 3(b)]. Moreover, local brightness contrast is displayed in the Ga- and N-face regions shown in Figs. 2 and 3. The bright spots in the images may be dissociated Ga islands, foreign material, or inversion domains.

To explore the electronic properties of the different regions, we obtained PEEM images with photon energies from 4.5 to 6.3 eV in steps of 0.1 eV (Fig. 4). We note again that the beam exhibits a Gaussian spectral distribution with a FWHM of $\sim$0.1 eV. For photon energies below 4.8 eV, contrast between the two regions was not detected [Fig. 4(a)]. However, for photon energies greater than 4.9 eV, emission from the N-face regions was observed, which led to a distinct emission contrast between the two domains [Fig. 4(b)]. As the photon energy was increased from 4.8 eV, the emission from the N-face regions also increased leading to enhanced contrast [Fig. 4(c)]. However, at 6.3 eV the emission from the Ga-face region became more significant, and the emis-

sion contrast was relatively reduced [Fig. 4(d)]. From the results, we can deduce that the photothreshold of N-face region is less than ~4.9 eV while that of the Ga-face regions is greater than 6.3 eV. Also, the bright emission from the IDBR indicates an emission threshold of less than 4.9 eV [Fig. 4(b)]. As the photon energy increased, the emission intensity of the IDBR increased significantly. However, the region of intense emission was only the N-face side of the IDBR.

IV. DISCUSSION

A. Polarity contrast between the Ga- and N-face surfaces

We consider first the origin of the difference in the photoemission yield from the Ga- and N-face regions. The photoelectric yield is strongly related to the photothreshold. For a semiconductor with flat bands at the surface, the photothreshold is equal to the sum of band gap and electron affinity. For the Ga-face GaN, photoemission studies have indicated an electron affinity of 2.9–3.6 eV depending on surface processing.[18–20] Then with the 3.4 eV band gap, the photothreshold is expected at 6.3–7.0 eV. Our measurements of the Ga-face regions show that emission is observed at photon energies of greater than 6.3 eV, which is consistent with this analysis.

It is evident that effects such as surface termination, surface reconstruction, adsorbate layers and atomic steps could significantly affect the electron affinity.[21] To our knowledge there are no photoemission measurements of the electron affinity of the different polarity surfaces of GaN, but we can obtain some insight into the electron affinity from measurements of the Schottky barrier. Current–voltage and photoresponse measurements indicate that the Schottky barrier for Pt on *n*-type GaN is larger on the Ga face than on the N face.[4] Then based on the Schottky–Mott model, we would expect that the electron affinity of the N face is larger than that of the Ga face. Thus, it seems unlikely that an electron affinity variation could explain the observed difference in emission intensity and threshold for the N- and Ga-face regions.

To explain the much lower photothreshold at the N-face surface, it is necessary to consider the effect of the polarity on the band structure at each surface. In *n*-type GaN, the energy band diagrams for the Ga- and N-face surfaces are illustrated in Fig. 5. The bulk Fermi level position can be determined using the relationship, $(E_c - E_F) = kT \ln(N_c/N_d)$, where k is the Boltzmann constant, N_d is the doping concentration and N_c is the effective density of states in the conduction band ($N_c = 2.6\times10^{18}$ cm^{-3}). The value of $(E_c - E_F)$ in the bulk of our GaN film is estimated to be ~0.05 eV below the conduction band edge for both Ga- and N-face regions.

For the Ga-face region, the spontaneous polarization (-0.034 C/m^2) points from the surface to the substrate, inducing a negative bound charge at the GaN surface ($\sigma/e = -2.12\times10^{13}$ cm^{-2}) and a positive bound charge of the same value at the GaN/substrate interface. We only consider the spontaneous polarization, which dominates the total polarization.[9] The negative bound charge at the surface is screened by the positively ionized donors close to the surface. This leads to upward band bending in the depletion region at the Ga-face surface [Fig. 5(a)]. In contrast, downward band bending should occur at the N-face surface due to the opposite direction of the spontaneous polarization. The positive bound surface charge gives rise to a free electron accumulation layer at the N-face surface, fixing the Fermi level close to the conduction band edge. In addition, if there are N vacancies in the film, the charged defects would act as donors,[22] and enhance the electron density of the electron accumulation layer. This accumulation layer leads to a slight downward bending of the conduction band edge at the N-face surface [Fig. 5(b)]. A theoretical calculation has indicated that the band bending difference between the Ga- and N-face surfaces could be equal to the band gap of ~3.4 eV in GaN.[4] However high-resolution photoemission measurements demonstrated a much lower value of 1.4 eV.[13] Also, experiments from our laboratory obtained a value of ~0.3 eV for upward band bending at CVC-treated Ga-face surfaces of GaN film grown on SiC using ultraviolet photoelectron spectroscopy.[23] These differences could be due to the compensation of polarization bound charges by adsorbed molecules, structural defects, or oxidation of the surfaces.

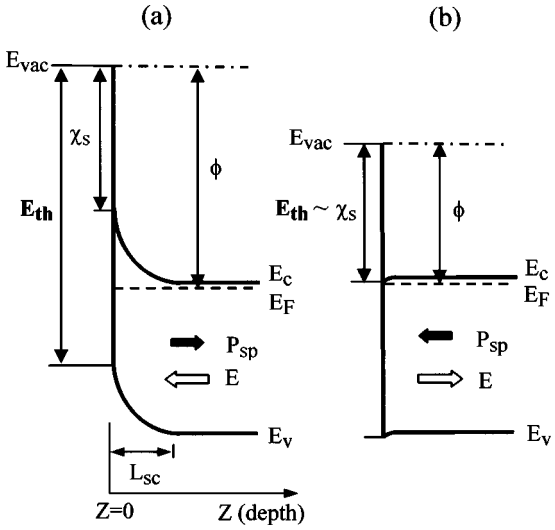

FIG. 5. Energy band diagrams for (a) Ga-face and (b) N-face GaN. The quantities χ_s, ϕ, E_{th}, and L_{sc} are the surface electron affinity, work function, photothreshold, and space charge layer, respectively. The arrows represent the directions of spontaneous polarization, P_{sp}, and the internal electric field, E.

The surface band bending gives rise to a variation in the photothreshold at the different polar surfaces. For upward band bending of the Ga-face region, the photothreshold at the bulk increases by the amount of band bending while the photothreshold at the surface does not change and is $\chi_s + E_g$ [Fig. 5(a)]. Thus, the electrons are photoemitted from the valence band edge at the surface for a photon energy greater than $\chi_s + E_g$. On the other hand, for downward band bending of the N-face region, an electron accumulation layer results in the conduction band minimum slightly below the Fermi level. As a result, the electrons in the accumulation layer can be photoemitted from the conduction band, and the photothreshold at the surface would be essentially the electron affinity [Fig. 5(b)]. Thus, the relatively bright intensity

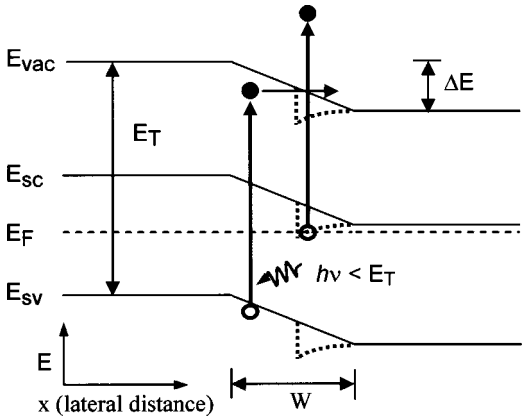

FIG. 6. Proposed lateral band diagram of the GaN surface in the vicinity of an IDB. The electron affinities of two faces surfaces are assumed to be equal. The excitation photon energy, $h\nu$, is greater than E_g and less than E_{th} $(=E_g+\chi)$. W is a lateral space charge region with the IDB located in the middle. The left side of W is the Ga face while the right side is N face. ΔE is the built-in potential energy induced by the band bending difference between Ga- and N-face GaN. The dotted lines represent the modified bands near the IDB ascribed to a band edge discontinuity.

at the N-face regions is attributed to electron emission from the conduction band due to downward band bending.

Therefore, the polarity dependent photothreshold causes a photoelectric yield difference between the Ga- and N-face regions and leads to the polarity contrast in the PEEM images of the GaN film.

Following this explanation, adsorbed ions at the as-loaded GaN surface can give rise to a compensation of the polarization charges on both polar surfaces. The charge compensation reduces the photoelectric yield difference induced by the band bending difference, which can explain why the polarity contrast could not be detected.

B. Intense emission from IDBRs

We now discuss possible emission mechanisms for the strong intensity at the IDBRs in the PEEM images. First, topographic effects due to the surface morphology of the sample could cause a local enhancement in electron emission.[11] Field enhancement from a feature with a relatively small radius of curvature or the Schottky effect at the top of a protruding feature can lead to enhanced emission intensity in PEEM. However, the AFM cross-section profile shows that the height and curvature variation across the IDBs are essentially negligible [Fig. 3(a)]. This indicates that the surface topography does not significantly affect the emission intensity. In addition, mezoscopic steps of ~ 2 μm width and ~ 10 nm height were observed between the Ga and N face regions for similar samples.[7] However, these steps have such a low aspect ratio that they would not be expected to enhance the PEEM emission.

Second, we can consider an additional photoexcitation process aside from the normal electron excitation from the valence band edge. The band bending difference between the Ga- and N-face surfaces can play a significant role which can lead to an additional emission process at the IDBRs. A lateral band diagram of a LPH surface in the vicinity of the IDB is illustrated in Fig. 6. For the N-face surface of an *n*-type GaN film, the Fermi level is close to the surface conduction band edge because the positive bound surface charge causes an electron accumulation layer at the surface. In contrast, for the Ga-face surface the E_F moves towards the surface valence band edge according to the degree of the upward band bending. Assuming no charged defects at the IDB; the band edges will shift from the Ga face to the N face across the IDB. Consequently, the potential energy difference results in a built-in lateral field and a surface space charge region. The built-in potential energy, ΔE, would be approximately equal to the band bending difference between Ga- and N-face regions, which is dependent upon the screening of the bound surface charges $(\Delta E \sim 1\ \text{eV})$.[13] The width of the space charge region into the bulk of GaN will be several μm where we have used the expression, $W=(2\varepsilon\Delta E/eN_d)^{1/2}$, and ε is dielectric constant of GaN and N_d is the density of polarization-induced surface charges. We could expect a similar width for the lateral depletion region. Using these values, a lateral electric field of ~ 10 kV/cm will be built-in on the surface near the IDB.

It is known that IDB exhibit local NaCl-like geometry, opposing the surrounding wurtzite structure.[5] However, the PEEM would not likely detect this atomic scale structural change due to the 10 nm resolution limit.

The structural transition region and the IDB can also contribute to the band structure. To draw the modified band diagram, we should solve Poisson's equation across the IDB, taking into account the details of the charge density throughout the IDBR and the polarization bound charge at both face surfaces. We have assumed that the sheet charge density of the *n*-type, N-face regions is larger than the polarization surface charge $(\sim 2\times 10^{13}\ \text{cm}^{-2})$, and we have included a band edge discontinuity at the IDB and a slight downward band bending from the N-face side of the IDBR. With these assumptions, we can sketch an approximate diagram without a detailed calculation as indicated by the dotted lines in Fig. 6.

On the basis of the lateral band diagram, we can postulate two mechanisms to account for the electron emission from the IDBRs (Fig. 6). First, for a photon energy greater than $(E_T-\Delta E)$ and less than $E_T(=\chi_s+E_g)$, the photoexcited electrons from the valence band maximum of the Ga-face side in the IDBR cannot be emitted into the vacuum. Instead, because of the built-in field some of the electrons will be able to traverse the IDB and diffuse into the N-face side in the IDBR. The diffused hot electrons at the N-face side can be emitted directly into the vacuum since they are above the vacuum level. Second, the electrons originating from the conduction band edge of the N-face side of the IDBR can directly contribute to the photoemission yield because of the downward band bending. Within our band schematic, it is apparent that the second process would have the lower photothreshold. Although both effects could contribute to the intense emission from the N-face side of the IDBR, we expect that the second mechanism is more dominant. More detailed studies of the IDB structure and electron affinity of the polar surfaces would be helpful in verifying the proposed IDBR emission mechanism.

V. CONCLUSIONS

We have used UV-PEEM to image emission from a GaN-based LPH. Polarity contrast was observed between the Ga- and N-face regions as well as intense emission from the IDBR. The enhanced emission from the N-face surface is attributed to photoemission from electrons in the conduction band at the surface induced by band bending. We propose that the intense emission from the IDBR is predominantly due to emission of electrons in an accumulation layer in the conduction band, but emission of hot electrons diffused by the laterally built-in field may also contribute. The proposed surface energy bands of the LPH are similar to that of a *p-n* heterojunction device and could exhibit rectifying behavior for electronic transport across the IDB.

ACKNOWLEDGMENTS

The authors gratefully acknowledge the Duke Free Electron Laser Laboratory for access to the OK-4 Free Electron Laser. This work was supported by grants through the MFEL Program administered through the AFOSR, and the Office of Naval Research MURI on Polarization Electronics, Contract No. N00014-99-1-0729.

[1] O. Ambacher, J. Smart, J. R. Shealy, N. G. Weimann, K. Chu, M. Murphy, R. Dimitrov, L. Wittmer, M. Stutzmann, W. Rieger, and J. Hilsenbeck, J. Appl. Phys. **85**, 3222 (1999).
[2] M. Stutzmann, O. Ambacher, M. Eickhoff, U. Karrer, A. Lima Pimenta, R. Neuberger, J. Schalwig, R. Dimitrov, P. Schuck, and R. Grober, Phys. Status Solidi B **288**, 505 (2001).
[3] E. S. Hellmann, MRS Internet J. Nitride Semicond. Res. **3**, 11 (1998).
[4] U. Karrer, O. Ambacher, and M. Stutzmann, Appl. Phys. Lett. **77**, 2012 (2000).
[5] V. Fiorentini, Appl. Phys. Lett. **82**, 1182 (2003).
[6] J. E. Northrup, J. Neugebauer, and L. T. Romano, Phys. Rev. Lett. **77**, 103 (1996).
[7] V. Cimalla and O. Ambacher, M. Eickhoff, C. Miskys, M. Stutzmann, B. J. Rodriquez, R. Nemanich, M. Drakopoulos, and J. Zegenhagen, presented at the International Workshop on Nitride Semiconductors 2002, Aachen, Germany (unpublished).
[8] P. J. Schuck, M. D. Mason, R. D. Grober, O. Ambacher, A. P. Lima, C. Miskys, R. Dimitrov, and M. Stutzmann, Appl. Phys. Lett. **79**, 952 (2001).
[9] B. J. Rodriguez, A. Gruverman, A. I. Kingon, R. J. Nemanich, and O. Ambacher, Appl. Phys. Lett. **80**, 4166 (2002).
[10] M. Park, J. J. Cuomo, B. J. Rodriguez, W.-C. Yang, R. J. Nemanich, and O. Ambacher, J. Appl. Phys. **93**, 9542 (2003).
[11] H. Ade, W. Yang, S. English, J. Hartman, R. F. Davis, R. J. Nemanich, V. N. Litvinenko, I. V. Pinayev, Y. Wu, and J. M. Mady, Surf. Rev. Lett. **5**, 1257 (1998).
[12] V. W. Ballarotto, K. Siegrist, R. J. Phaneuf, E. D. Williams, W.-C. Yang, and R. J. Nemanich, Appl. Phys. Lett. **78**, 3547 (2001).
[13] H. Jang, J. H. Lee, and J. L. Lee, Appl. Phys. Lett. **80**, 3955 (2002).
[14] R. Dimitrov, V. Tilak, M. Murphy, W. J. Schaff, L. F. Eastman, A. P. Lima, C. Miskys, O. Ambacher, and M. Stutzmann, Mater. Res. Soc. Symp. Proc. **622**, T4.6.1 (2000).
[15] S. W. King, J. P. Barnak, M. D. Bremser, K. M. Tracy, C. Ronning, R. F. Davis, and R. J. Nemanich, J. Appl. Phys. **84**, 5248 (1998).
[16] A. J. McGinnis, D. Thomson, R. F. Davis, E. Chen, A. Michel, and H. H. Lamb, J. Cryst. Growth **222**, 452 (2001).
[17] G. F. Rempfer and O. H. Griffith, Ultramicroscopy **27**, 273 (1989).
[18] S. P. Grabowski, M. Schneider, H. Nienhaus, W. Monch, R. Dimitrov, O. Ambacher, and M. Stutzmann, Appl. Phys. Lett. **78**, 2503 (2001).
[19] C. I. Wu, A. Kahn, N. Taskar, D. Dorman, and D. Gallagher, J. Appl. Phys. **83**, 4249 (1998).
[20] P. J. Hartlieb, A. Roskowski, R. F. Davis, W. Platow, and R. J. Nemanich, J. Appl. Phys. **91**, 732 (2002).
[21] R. J. Nemanich, *GaN and Related Semiconductors*, edited by J. H. Edgar *et al.* (INSPEC, London, 1999), p. 98.
[22] D. C. Look, D. C. Reynolds, Z.-Q. Fang, J. W. Hemsky, J. R. Sizelove, and R. L. Jones, Mater. Sci. Eng., B **66**, 30 (1999).
[23] K. M. Tracy, W. J. Mecouch, R. F. Davis, and R. J. Nemanich, J. Appl. Phys. **94**, 3163 (2003).